Published in final edited form as:
*J Neurosci Res*. 2013 March ; 91(3): 393–406. doi:10.1002/jnr.23169.

# Sulindac Sulfide Inhibits Sarcoendoplasmic Reticulum $Ca^{2+}$ ATPase, Induces Endoplasmic Reticulum Stress Response, and Exerts Toxicity in Glioma Cells: Relevant Similarities To and Important Differences From Celecoxib

**M.C. White**[1], **G.G. Johnson**[1], **W. Zhang**[2], **J.V. Hobrath**[2], **G.A. Piazza**[3], and **M. Grimaldi**[1,*]

[1]Laboratory of Neuropharmacology, Medicinal Chemistry Department, Drug Discovery Division, Southern Research Institute, Birmingham, Alabama

[2]Molecular Modeling Laboratory, Medicinal Chemistry Department; Drug Discovery Division, Southern Research Institute, Birmingham, Alabama

[3]Drug Discovery Research Center, Mitchell Cancer Institute, University of South Alabama, Mobile, Alabama

## Abstract

Malignant gliomas have low survival expectations regardless of current treatments. Nonsteroidal anti-inflammatory drugs (NSAIDs) prevent cell transformation and slow cancer cell growth by mechanisms independent of cyclooxygenase (COX) inhibition. Certain NSAIDs trigger the endoplasmic reticulum stress response (ERSR), as revealed by upregulation of molecular chaperones such as GRP78 and C/EBP homologous protein (CHOP). Although celecoxib (CELE) inhibits the sarcoendoplasmic reticulum $Ca^{2+}$ ATPase (SERCA), an effect known to induce ERSR, sulindac sulfide (SS) has not been reported to affect SERCA. Here, we investigated these two drugs for their effects on $Ca^{2+}$ homeostasis, ERSR, and glioma cell survival. Our findings indicate that SS is a reversible inhibitor of SERCA and that both SS and CELE bind SERCA at its cyclopiazonic acid binding site. Furthermore, CELE releases additional $Ca^{2+}$ from the mitochondria. In glioma cells, both NSAIDS upregulate GRP78 and activate ER-associated caspase-4 and caspase-3. Although only CELE upregulates the expression of CHOP, it appears that CHOP induction could be associated with mitochondrial poisoning. In addition, CHOP induction appears to be uncorrelated with the gliotoxicity of these NSAIDS in our experiments. Our data suggest that activation of ERSR is primarily responsible for the gliotoxic effect of these NSAIDS. Because SS has good brain bioavailability, has lower COX-2 inhibition, and has no mitochondrial effects, it represents a more appealing molecular candidate than CELE to achieve gliotoxicity via activation of ERSR.

### Keywords

GRP78; gliotoxicity; $Ca^{2+}$; NSAIDs

Malignant gliomas (MG) are poorly sensitive and quickly develop resistance to treatments. The survival rates are dismal, and the median survival from diagnosis is less than 1 year



*Correspondence to: Dr. Maurizio Grimaldi, Laboratory of Neuropharmacology, Department of Biochemistry and Molecular Biology, Drug Discovery Division, Southern Research Institute, 2000 9th Avenue South, Birmingham, AL 35205. grimaldi@southernresearch.org.

(Shrieve et al., 1999). Over the last 3 decades, nonsteroidal anti-inflammatory drugs (NSAIDs) have been linked to inhibition of carcinogenesis in many types of cancers (Rao and Reddy, 2004; Cerchietti et al., 2005). Additionally, radiation or chemotherapy coupled with administration of NSAIDs results in better outcomes in MGs (Shono et al., 2001; Cerchietti et al., 2005; Tuettenberg et al., 2005; Wagemakers et al., 2009). Unfortunately, the antineoplastic effects of NSAIDs are achieved at high doses, which can cause life-threatening complications.

It was initially hypothesized that the antitumor effects of NSAIDS were due to inhibition of cyclooxygenase (COX). However, analogs of NSAIDs devoid of COX inhibition are as effective as the original NSAIDs. Examples of this are 2,5-dimethylcelecoxib (DMC; Pyrko et al., 2006; Schonthal, 2006) and dimethylaminoethyl amide derivatives of sulindac (Piazza et al., 1995). Thus, the antineoplastic effects of NSAIDs occur independently of COX inhibition (Piazza et al., 1995; Kardosh et al., 2005; Chuang et al., 2008).

Certain NSAIDs such as DMC and celecoxib (CELE) induce the endoplasmic reticulum stress response (ERSR) and result in cytotoxicity (Chuang et al., 2008; Kardosh et al., 2008; Chen et al., 2009). Most likely, ERSR induction by these agents is due to blockade of sarcoendoplasmic reticulum $Ca^{2+}$-ATPase (SERCA), as shown in PC-Cl3 cells (Johnson et al., 2002).

The ER, the main fast-acting reservoir of $Ca^{2+}$ (Koch, 1990), is also a site for protein assemblage, sorting, storing, and shipping (Hussain and Ramaiah, 2007). In the ER, $Ca^{2+}$-dependent chaperones direct folding and transport of newly synthesized proteins. The $Ca^{2+}$-pump, SERCA, solely maintains the high concentration of $Ca^{2+}$ required for signaling and protein folding. When the ER is unable to maintain high $Ca^{2+}$ concentrations, defects in signaling and protein folding occur, activating the ERSR. The proteins initiating ERSR include activating transcription factor 6 (ATF6), PKR-like ER kinase (PERK), inositol-requiring kinase 1 (IRE1), and ER-associated caspases (−4 in human and −12 in rat), which are bound to and kept inactive by GRP78. When unfolded proteins (UP) accumulate in the ER, they bind to GRP78 with high affinity and cause the release/activation of the aforementioned factors (Kim et al., 2008). Release of such ERSR-initiating proteins from GRP78 leads to deployment of the ERSR (Xu et al., 2005). Increased expression of the chaperones and SERCA increases the ability to fold proteins. Concomitant protein synthesis inhibition and activation of protein degradation via the ER-associated protein degradation (ERAD) system decreases the ER protein load. Finally, ERSR can trigger cell death mostly via apoptosis (Ogata et al., 2006; Egger et al., 2007).

Given reports that CELE acts as a SERCA inhibitor, interferes with $Ca^{2+}$ influx, and induces the activation of ERSR (Johnson et al., 2002; Kardosh et al., 2008), we initiated a systematic investigation of NSAID effects to determine their potential as ERSR-inducers in MG cells. We sought to characterize the role of $Ca^{2+}$ homeostatic disturbances by SS and other NSAIDs and their relationship with ERSR induction and cytotoxicity. We investigated CELE (a COX2 inhibitor) and sulindac sulfide (SS; a COX1 inhibitor with modest effects on COX2) for their effects on $Ca^{2+}$ homeostasis, ERSR, and MG cell survival. We report for the first time that, in MG cells, SS is a SERCA inhibitor, induces ERSR, and causes cell death by activation of ER-associated caspase-4 and thus caspase-3. We also demonstrate that CELE affects mitochondria. Because SS and CELE result in similar levels of cytotoxicity, we conclude that ERSR induction is uniquely responsible for their toxic effect on MG cells.

# MATERIALS AND METHODS

## Reagents

Commercial samples of Celebrex capsules (Pfizer, NY) were kindly provided by Dr. FredWhite. All other reagents were purchased from Sigma (St. Louis, MO), unless noted otherwise.

## Cell Cultures

C6 and U87-MG (MG) glioma cells were purchased from the American Tissue Culture Collection (Rockville, MD). Both cells types were expanded and frozen (passages 1–5). Thawed cells were cultured in high-glucose Dulbecco's modified Eagle's medium (DMEM; Gibco, Grand Island, NY) containing 10% heat-inactivated fetal bovine serum (FBS) and penicillin/streptomycin (Invitrogen, Carlsbad, CA). The cells were used between passages 5 and 25.

## Single-Cell $[Ca^{2+}]_i$ Measurements

Cells were seeded on glass coverslips (Assistant, Germany) at 40,000 cells/$cm^2$ and allowed to attach overnight. This higher density yields a sufficient number of cells at the high magnification required for $Ca^{2+}$ imaging experiments. Cells were washed with Krebs-Ringer buffer (KRB) prepared in house and containing NaCl (125 mM), KCl (5 mM), $Na_2HPO_4$ (1 mM), $MgSO_4$ (1 mM), $CaCl_2$ (1 mM), glucose (5.5 mM), and HEPES (20 mM, pH 7.4), then loaded with 2 μm Fura-2AM (Molecular Probes, Eugene, OR) in KRB for 22 min at RT to minimize compartmentalization of the probe (Roe et al., 1990). Subsequently, coverslips were washed once with KRB, mounted in a self-built perfusion chamber (150 μl), and perfused with either $Ca^{2+}$-containing or $Ca^{2+}$-free KRB (containing 100 μM EGTA) at ~1 ml/min. An inverted, customized microscope (model IX50; Olympus, Center Valley, PA) was used to observe the preparations. The microscope was equipped with a computer controlling the emission and excitation mechanical filter changers and a high-speed camera. The software Metafluor (Molecular Devices, Sunnyvale, CA), was used to coordinate hardware functions, image acquisition, and image analysis.

Image pairs collected every 2 sec, with excitation switching between 340 nm and 380 nm and emission set at 510 nm, were used to generate ratio images. Regions of interest were drawn by delineating the cell profile to obtain average ratio values. Values obtained at matching time points for all cells were averaged and used to generate graphs and to perform statistical analyses.

## Viability Assay

MG and C6 cells were plated at a low density of 10,000 cells/well and 8,000 cells per well, respectively, in a white-walled 96-well plate. Such a number of cells allows ample margin for cell growth over 72 hr. After a 48-hr treatment with the compounds, cells were assessed for viability by using Cell Titer Glo (Promega, Madison, WI) according to the manufacturer's instructions. Each concentration was tested in quadruplicate on three separate cell preparations.

## Western Blotting

Cells were lysed in a buffer consisting of 20 mM Tris-HCl (pH 7.5, 150 mM NaCl, 1 mM EGTA, 1% Triton X-100, 2.5 mM sodium pyrophosphate, 1 mM glycerol phosphate, 1 mM $Na_3VO_4$, 1 μg/ml leupeptin, and 1 mM phenyl-methylsulfonyl fluoride; Cell Signaling, Beverly, MA). After brief sonication, lysates were clarified by centrifugation at 12,000 rpm for 12 min at 4°C, and protein content in the supernatant was measured according to the

bicinchoninic method (Pierce, Thermo Scientific, Rockford, IL). Aliquots (100 μg of protein per lane) of total protein were separated by 10% SDS-PAGE and blotted onto nitrocellulose transfer membranes (Fisher Scientific, Pittsburgh, PA). Each membrane was blocked with 5% nonfat dry milk in TBS-T (20 mM Tris-HCl, pH 7.5, 137 mM NaCl, and 0.01% Tween-20) for 1 hr at room temperature. Appropriate primary antibodies were incubated overnight at 4°C. After gently washing with TBS-T, each membrane was incubated with horseradish peroxidase-conjugated anti-rabbit (catalog No. PI-31462; Fisher Scientific) or anti-mouse (catalog No. PI-31430; Fisher Scientific) secondary antibodies (1:500–20,000) for 1 hr at room temperature in TBS-T containing 5% nonfat dry milk. Detection was performed using an enhanced chemiluminescence reagent (Fisher Scientific), according to the manufacturer's protocol. Densitometric analysis was performed in ImageJ software.

The following antibodies were used: GRP78 (1:1,000; catalog No. sc-13968; Santa Cruz Biotechnology, Santa Cruz, CA) and CHOP (1:1,000; catalog No. sc-7351; Santa Cruz Biotechnology), caspase-4 (1:500; catalog No. C3392; Sigma), caspase-3 (1:150; catalog No. 9661; Cell Signaling), and GAPDH (1:10,000; catalog No. 2118; Cell Signaling).

### Docking Analysis

For modeling and docking/scoring predictions, the Schrodinger software package was used. After replacement of the single amino acid L423V, the inositol triphosphate ($InsP_3$) receptor crystal structure (PDB ID: 1N4K) was relaxed through restrained energy minimization utilizing Impact tools of Protein Preparation Refinement, as implemented in the Schrodinger software package. For ligand docking, the Induced Fit Docking (IFD) protocols were used (Schrodinger), allowing side-chain flexibility within 5 Å of ligand atom groups. The center of the pocket was defined based on residues 250, 263, 265, 414, 505, 511, and 512, and the box-size parameter was set to 20. Based on the SERCA crystal structure (PDB ID: 2EAT), the same energy minimization and ligand-docking protocols were used to explore SERCA–ligand interactions.

### Statistical Analysis

Experiments were performed at least three times with different cell preparations at different cell passages. Results are presented as average values ± SE. For all experiments, statistical validation was performed by *t*-test. By convention, $P \leq 0.05$ indicated a statistically significant difference.

## RESULTS

### Effect of NSAIDs on $[Ca^{2+}]_i$

Graded concentrations of NSAIDs were tested for their effect on $[Ca^{2+}]_i$ in C6 cells using fura-2 single-cell imaging. Ibuprofen (IBU), even at a concentration of 400 μM, did not significantly affect $[Ca^{2+}]$i (Fig. 1A). In contrast, CELE and SS caused a marked, concentration-dependent increase of $[Ca^{2+}]_i$ (Fig. 1B,C). The effect of SS was similar in magnitude to the effect of CELE. For comparison, the effect of THAP (200 nM), an irreversible SERCA inhibitor (Thastrup et al., 1987), on $[Ca^{2+}]_i$ is provided (Fig. 1D). Agent removal from the perfusion medium terminated the effect of SS and CELE on $[Ca^{2+}]_i$, indicating the reversibility of the effects.

### SS and CELE Release $Ca^{2+}$From Intracellular $Ca^{2+}$Stores

To determine the source of $Ca^{2+}$ responsible for the SS and CELE effects, C6 cells were exposed to the NSAIDS in the absence of extracellular $Ca^{2+}$. Both SS and CELE increased $[Ca^{2+}]_i$, even in the absence of extracellular $Ca^{2+}$ (Fig. 2A, B). Under these conditions, elevation of $[Ca^{2+}]_i$ can occur only via release from intracellular $Ca^{2+}$ stores (ICS). For

comparison, the effect of THAP (200 nM) is shown in Figure 2C. The similarity between the $[Ca^{2+}]_i$ elevation recorded in response to the NSAIDS in the presence or absence of extracellular $Ca^{2+}$ (Fig. 2D) indicates that the ICS are the main source of the $[Ca^{2+}]_i$ increase caused by SS and CELE.

### Identification of the ICS Targeted by SS and CELE

To determine the intracellular source of $Ca^{2+}$ mobilized by SS and CELE, THAP was utilized to deplete ER stores in the absence of extracellular $Ca^{2+}$ before exposing the cells to the NSAIDs. In control experiments in which ER stores are depleted with THAP, subsequent treatment with THAP or ATP has been shown to elicit no further $Ca^{2+}$ response (Sabala et al., 1997; Grimaldi et al., 2003; Grimaldi, 2006). After treatment with THAP, SS caused no elevation of $[Ca^{2+}]_i$ in C6 (Fig. 3A), implicating the ER as the sole source of $Ca^{2+}$ mobilized by SS. When similar experiments were conducted with CELE, a residual $Ca^{2+}$ elevation was evident following THAP pretreatment, even though the effect of CELE was reduced by approximately 70% (Fig. 3B). Thus, CELE, in addition to causing release of $Ca^{2+}$ from the ER, affects additional ICS.

Because the mitochondria represent another large but slower-releasing store of $Ca^{2+}$, the possibility that the mitochondria could be an additional CELE target was evaluated. Carbonyl cyanide 4-(trifluoromethoxy)-phenylhydrazone (FCCP) is a protonophore that uncouples oxidative phosphorylation and collapses mitochondrial membrane potential (Haak et al., 2002). Exposure to FCCP has been shown to produce a progressive $Ca^{2+}$ release from the mitochondria and gradual depletion of $Ca^{2+}$ (Heytler, 1979). As a control, C6 cells were perfused with THAP and subsequently perfused with FCCP to verify that ER and mitochondrial $Ca^{2+}$ were independently targeted by THAP and FCCP (data not shown). C6 cells were perfused in a $Ca^{2+}$-free KRB; THAP and FCCP were applied to deplete the ER and the mitochondria simultaneously. When $[Ca^{2+}]_i$ stabilized near baseline levels, the cells were then exposed to CELE. Under these conditions, the effect of CELE was inhibited by more than 90% (Fig. 3C). It is likely that the residual effect of CELE is due to leakage of residual $Ca^{2+}$ present in the mitochondria. A comparison of the $[Ca^{2+}]_i$ responses to CELE following the different conditions is provided in Figure 3D.

Because SS causes $Ca^{2+}$ release from the ER, we attempted to identify its mechanism of action. $Ca^{2+}$ exits the ER in two main ways: activation of the inositol triphosphate receptors ($InsP_3R$) and passive loss. The latter is due to the driving force constituted by the high ER $Ca^{2+}$ concentration (100 μM) relative to the low levels in the cytoplasm (70–100 nM). This ion loss is usually counteracted by SERCA activity.

One method to examine the effect of a compound on the $InsP_3R$ is using one of its known inhibitors. Unfortunately, only a few specific $InsP_3R$ inhibitors exist, and those commonly used are difficult, unreliable, and have questionable selectivity. In fact, they are often responsible for unexpected effects on $Ca^{2+}$ homeostasis (Bootman et al., 2002), which can differ between cell lines. Our group has been successful in preventing the effect of ATP, an agent increasing $InsP_3$ in primary astrocytes, by use of 2-aminoethoxydiphenyl borate (2-APB; Grimaldi et al., 2003). Therefore, C6 cells were exposed to 2-APB to determine whether the SS effect could be ascribed to $InsP_3$-mediated $Ca^{2+}$ mobilization from the ER. Preliminary experiments with C6 cells exposed to 2-APB revealed that this agent induced an elevation of $[Ca^{2+}]_i$ that resembles that of THAP (data not shown), an effect not seen in astrocytes (Grimaldi et al., 2003). Followup experiments (data not shown) suggested that 2-APB could affect SERCA function in C6 cells, as previously reported for other cell types (Bilmen et al., 2002). Therefore, 2-APB could not be used to study a potential effect of SS on the $InsP_3R$ in C6 cells. In lieu of the unfeasible pharmacological $InsP_3R$ blockade, an alternative experiment was designed to determine whether $InsP_3R$ was involved in SS

action. We exposed C6 cells simultaneously to a maximal ATP concentration (Grimaldi et al., 1999) and to SS. We hypothesized that, if SS affects the $InsP_3R$, the response to a maximal ATP concentration would not be affected since ATP already would be maximally activating $InsP_3$ production. If SS affects another target, then the ATP response would be modified according to the target affected. Extracellular ATP has been extensively studied in glioma cells for release of $Ca^{2+}$ from the ER. Whereas a concentration-dependent increase of $[Ca^{2+}]_i$ occurs with ATP, release of maximal ER $Ca^{2+}$ stores in C6 cells occurs at about 20 μM (Sabala et al., 1997). For this reason, we used a supramaximal dose of 100 μM ATP to elicit without a doubt a maximal ATP response. When cells were treated with ATP and SS, the ATP effect was significantly modified (Fig. 4A). In particular, both the peak and the plateau phase were increased, indicating that the balance between $Ca^{2+}$ influx and $Ca^{2+}$ reuptake into the ER could have been altered by SS (Moller, 2002). The experiments in Figure 2A showed that SS had no effect on $Ca^{2+}$ influx, so SS must alter $Ca^{2+}$ reuptake in the ER. Additionally, the profile of the effect of ATP + SS resembles the profile of the effect of ATP + THAP (Fig. 4A). These results suggest that SS does not cause release of $Ca^{2+}$ from the ER by affecting the $InsP_3R$ but rather via a THAP-like action, as in the case of CELE (Johnson et al., 2002; Kardosh et al., 2005, 2008). The peak and plateau responses for all experimental conditions are analyzed in Figure 4B.

To strengthen the view that SS is not affecting the $InsP_3$-regulated ER $Ca^{2+}$ efflux, *in silico* docking of SS to the $InsP_3R$ was performed to determine whether SS had the potential to bind this receptor. The mouse $InsP_3R$ structure is available at 2.2-Å resolutions (PDB entry code 1N4K). We mutated the structure at a single residue to obtain the human sequence (L423V). After an initial energy minimization to relax the structure, IFD protocols were used (from Schrodinger) for docking SS into the active site of $InsP_{3R}$, which allows side-chain flexibility within 5 Å from ligand atom groups. The available pocket is large enough to accommodate SS in two possible docked poses, as illustrated in Figure 4C, where SS carbons are colored light brown. The position of $InsP_3$ is shown in the crystal structure. The only favorable interactions present in these two docked SS poses are salt-bridging interactions between the carboxylate group and surrounding arginines. The other parts of SS are nonpolar. These are surrounded by polar residues in this pocket, and there are no favorable interactions in either of the two poses. This predominantly polar pocket is also mostly exposed on the surface to the solvent and, therefore, it is not suitable to accommodate nonpolar atom groups, such as those in SS. We conclude that the docking program is capable of fitting SS near $InsP_3$ into the active site driven by favorable salt-bridging interactions involving a single group, the carboxylate; no other favorable interactions are present. In this solvent-exposed, polar site, the nonpolar atom groups of the SS structure are a “mismatch.” Thus, such poses may be predicted, but are unrealistic, and SS is unlikely to interact with the $InsP_3R$.

## SS and CELE Likely Bind to the Cyclopiazonic Acid Site of SERCA

Based on our data indicating that SS interferes with ER $Ca^{2+}$ reuptake and previously published data linking CELE to SERCA inhibition (Johnson et al., 2002), molecular docking studies were performed to explore the potential interactions between SS, CELE, and SERCA. Molecular modeling was accomplished with the built-in modules of Schrodinger Suite 2010. The SERCA protein structures were obtained from the protein databank (PDB ID: 2EAT) and optimized with the protein preparation wizard. The IFD protocol, which takes into consideration ligand-induced receptor conformational changes, was used in all docking studies. Residues within 5 Å of the ligands were allowed to be flexible. The docking results were scored using the extraprecision (XP) mode of Glide. The IFD protocol and parameters were first validated by docking cyclopiazonic acid (CPA) and THAP separately to their binding sites on SERCA. The docked results reproduced binding

conformations of CPA and THAP, as in the complex crystal structure (not shown). Because both the CPA and the THAP sites of SERCA are potential binding sites for SS and CELE, two parallel docking studies targeting either the THAP or the CPA site (Fig. 4D and E, respectively) were performed. CPA and THAP were included as controls. The docking results predict that the CPA binding site is energetically more favorable, relative to the THAP site, for binding of SS and CELE (Fig. 4F).

## ERSR Is Differentially Deployed in Response to SS and CELE

In many cell types, including MG cells, depletion of ER $Ca^{2+}$ similar to that induced by THAP has been associated with protein unfolding and induction of ERSR (Kim et al., 2008). Therefore, it is plausible that agents acting like THAP, in this case SS and CELE, could induce ERSR. The previous $Ca^{2+}$ experiments utilized C6 rat glioma cells because of culture ease and reliability in $Ca^{2+}$ imaging. For evaluation of the ERSR in response to CELE and SS, we utilized U87-MG (MG) human glioma cells to better understand the translational effects of these compounds. However, similar results were obtained in C6 (not shown). MG cells were exposed to 100 μM CELE, 150 μM SS, 1 μM FCCP, SS + FCCP, or 200 nM THAP, and expression of key proteins involved in the ERSR cascade were evaluated. IBU was not evaluated for activation of ERSR since no effect on $Ca^{2+}$ was seen in the previous experiments. The SS + FCCP treatment was included to mimic the effect of CELE based on our data obtained in Fura-2 $Ca^{2+}$ monitoring studies, which suggest that CELE also causes the release of $Ca^{2+}$ from the mitochondria. Protein levels of GRP78, the main sensor of protein unfolding and actuator of ERSR, were elevated following exposure of cells for 18 hr to THAP, SS, SS + FCCP, and CELE (Fig. 5A). Conversely, FCCP did not cause any increase in GRP78 (Fig. 5A). SS, CELE, and THAP resulted in 4.5-, 7.5-, and 8-fold inductions of GRP78, respectively. Addition of FCCP to the SS treatment had no appreciable effect on the induction of GRP78 compared with SS alone; both caused approximately a fourfold induction of GRP78. Additionally, the effect of CELE was not significantly different from that of SS or SS + FCCP. These data indicate that ERSR induction following NSAIDs exposure is unrelated to the mitochondrial poisoning caused by FCCP or CELE. Another molecule involved in ERSR deployment, CHOP, was induced only in cells exposed to SS + FCCP or CELE for 18 hr and not in cells exposed to SS, THAP, or FCCP alone (Fig. 5B). CELE, but not FCCP, caused an induction in CHOP expression, indicating that mitochondrial perturbation accompanied by ERSR is necessary to induce CHOP expression, an unexpected finding. This feature has not been previously reported. To the best of our knowledge and in accordance with our results, FCCP treatment has not been shown to induce CHOP. Additionally, ERSR activated by SS- and THAP-induced ER $Ca^{2+}$ depletion is not coupled to the expected increase of CHOP expression in glioma cells, as shown in other cellular systems.

## SS and CELE Trigger Apoptosis by Activating ER-Associated Caspases

Activation of apoptosis is a possible consequence of ERSR activation. Apoptosis driven by ERSR can be executed through ER-associated caspases and/or mitochondrial caspases (Hussain and Ramaiah, 2007). Although both pathways can converge to activate caspase-3, they can also operate independently to activate caspase-3. Converted caspases-4 and −3 cleaved from the inactive procaspase form were observed after 18 and 24 hr of exposure to NSAIDS. Activation of caspases was more pronounced at 24 hr, so only the 24 hr time point data is shown. Cleavage/activation of human-specific ER-associated caspase-4 occurred in MG cells treated for 24 hr with SS, SS + FCCP, CELE, and THAP but not in cells treated with FCCP alone (Fig. 5C). Caspase-4 cleavage was similar for each of these treatments, reaching approximately a threefold induction. Cleavage of caspase-3 occurred in MG cells exposed for 24 hr to CELE, THAP, SS, or SS + FCCP. As with the results for caspase-4, the cleavage of caspase-3 did not occur in cells exposed to FCCP (Fig. 5D). These data suggest

that mitochondrial poisoning with FCCP does not activate ERSR or induce caspase-3 activation. However, cleavage of caspase-3 was lower in response to SS treatment, compared with the CELE and SS + FCCP treatments, both of which were inducers of CHOP. Heightened CHOP activity and caspase-3 cleavage typically coincide, because knockdown of CHOP has previously been shown to reduce caspase-3 activity significantly in glioma cells (Thastrup et al., 1990; Kang et al., 2011). Although cleavage of caspase-4 was unaffected by mitochondrial poisoning, caspase-3, one of the final actuators of apoptosis, increased when mitochondrial function was affected, possibly reflecting the contribution of CHOP to caspase-3 activation (Fig. 5D).

### NSAIDs Are Cytotoxic to Glioma Cells

CELE and SS were tested for their effects on survival in C6 and MG cells to verify similar responses to CELE and SS in both cell types. After 48 hr of exposure to graded concentrations of IBU, SS, and CELE, cells were evaluated for viability by the glucose hexokinase assay and the Cell Titer Glo cytotoxicity kit. Although similar results were recorded with both detection systems, only data obtained with the Cell Titer Glo cytotoxicity kit are reported here. IBU showed less than 10% toxicity to glioma cells even at the highest tested concentration of 600 μM (data not shown). SS caused a concentration-dependent viability reduction in both C6 and MG, which was obtained in the range of concentrations evoking the effect on ERSR and on $Ca^{2+}$. The maximal viability reduction induced by SS, exceeding 85%, was reached at 200 μM in MG and at 400 μM in C6 cells (Fig. 6A). The $EC_{50}$ was calculated at approximately 150 μM of the compound. Similarly, CELE also caused a large viability reduction in both cell types. The maximal viability reduction exceeded 90% and was reached at 300 μM of CELE in both cell types (Fig. 6B). The $EC_{50}$ was calculated at approximately 80 μM of the compound.

## DISCUSSION

Investigations into the antitumor effects of NSAIDs began nearly 30 years ago (for review see Baron, 2003; Rao and Reddy, 2004; Cuzick et al., 2009). In contrast, it has been reported that treatment with an NSAID as a single agent has yet to cure any form of cancer (Ghosh et al., 2010). Despite this apparent drawback, NSAIDs, especially CELE, have been used in conjunction with radiation and chemotherapy in phase I/II clinical trials in MG. The results from these studies indicated that the combination of NSAIDs with conventional therapies was advantageous (Reardon et al., 2005; Grossman et al., 2008; Kesari et al., 2008). Early studies indicated that the beneficial effects of NSAIDs were caused by inhibition of COX and were based on the principle that prostaglandin E2 and other COX-generated mediators promote tumor growth (Jaffe, 1974; Kardosh et al., 2004). However, it is now clear that the antineoplastic effects of NSAIDs are the result of an as yet unidentified property. Recent evidence, however, suggests that additional mechanisms, including ERSR induction, may be involved or even entirely responsible for the anticancer effects of NSAIDs (Johnson et al., 2002; Tsutsumi et al., 2004; Chuang et al., 2008; Kardosh et al., 2008). Furthermore, it has been shown that COX-2 inhibition is neither necessary nor sufficient for the antiglioma effect exerted by NSAIDs (Chuang et al., 2008). Identification of the target responsible for these effects of NSAIDS is paramount, because, once such a target is identified, a drug development program could be launched and result in more effective and less toxic molecules.

Certain NSAIDs have been previously investigated for their effects on $Ca^{2+}$. The NSAIDs that affect $Ca^{2+}$ are associated with greater cytotoxicity to cancer cells (Tanaka et al., 2005). Although numerous reports document that CELE alters $Ca^{2+}$ homeostasis, reports on SS have been contradictory, showing either no effect on $Ca^{2+}$ in some cells (Pyrko et al., 2007) or inhibition of store-operated $Ca^{2+}$ entry (SOCE) in other cell types (Weiss et al., 2001). As

established in this report, CELE and SS cause an elevation of $[Ca^{2+}]_i$ in MG cells. In addition, our results indicate that CELE and SS release $Ca^{2+}$ exclusively from intracellular sources, because extracellular $Ca^{2+}$ withdrawal did not alter their effects. Upon depletion of the THAP-sensitive stores, mainly the ER, and in the absence of extracellular $Ca^{2+}$, the resulting reduction of their effects shows that both CELE and SS target ER $Ca^{2+}$. Because the effect of SS on $Ca^{2+}$ is completely inhibited by the simultaneous withdrawal of extracellular $Ca^{2+}$ and depletion of the ER, we conclude that SS releases $Ca^{2+}$ from the ER. To our knowledge, this is the first report documenting a THAP-like, selective, and reversible effect of SS. Our experiments also indicate that CELE, in addition to releasing $Ca^{2+}$ from the ER, targets other ICS, insofar as withdrawal of external $Ca^{2+}$ and depletion of the ER inhibited only 70% of its action. Our followup experiments clearly identify the mitochondria as the additional CELE target. Mitochondria poisoning is often regarded as a detrimental pharmacological property and definitely can be responsible for many of the unwanted adverse effects attributed to CELE. Our data may indicate a reason for the added clinical use liabilities of this particular drug.

Our *in silico* docking experiments support the hypothesis that SS and CELE could directly interact with SERCA on its inhibitory sites. Our data indicate that the CPA binding site, rather than the THAP site, is the most likely site of interaction. This hypothesis is also supported by the data shown in Figures 2A, B and 4A. In particular, the kinetics of $Ca^{2+}$ release from the ER are typical of uptake inhibition (i.e., SERCA inhibition) rather than release via the activation of the inositol trisphosphate receptor (cf. THAP and SS effect to ATP effect). Moreover, maximal $Ca^{2+}$ release via inositol trisphosphate elevation (ATP response in Fig. 4A) was not able to mask or prevent the action of SS, and the ATP + SS response resembles the ATP + THAP response, suggesting that SS has a THAP-like action rather than an ATP-like effect. Taken together, this evidence strongly suggests that the effect of SS is on ER $Ca^{2+}$ uptake rather than on ER $Ca^{2+}$ release. Although CELE has previously been shown to inhibit SERCA, we provide here the first documentation that CELE causes the release of $Ca^{2+}$ from mitochondria. Although an elevation of $[Ca^{2+}]_i$ in response to CELE in the presence of extracellular $Ca^{2+}$ has been previously reported for MG cells (Kardosh et al., 2008), a systematic investigation linking CELE to both SERCA inhibition and mitochondrial $Ca^{2+}$ loss has not been previously reported. Our findings on $Ca^{2+}$ substantiate the hypothesis that CELE, in addition to the THAP-like effect, has a direct effect on mitochondrial $Ca^{2+}$ homeostasis, as previously suggested (Jendrossek et al., 2003; Tanaka et al., 2005).

Recent evidence has suggested that SS causes cell death via ERSR induction in colon cancer cells (Yang et al., 2010). In previous reports, activation of PERK and the resulting eukaryotic translation initiation factor 2a (eif2α) kinase activation resulted in upregulation of CHOP and NSAID activated gene-1 (NAG-1), which is necessary for induction of apoptosis in colon cancer cells. Our data, however, show that SS-treated MG cells activate ERSR as indicated by the increase of GRP78 expression, cleavage/activation of the ER-associated caspase-4, and resultant cleavage/activation of caspase-3; this is accomplished without activation of CHOP, which is commonly considered the main activator of apoptosis during ERSR (Tabas and Ron, 2011). When mitochondrial function was disturbed by using the mitochondrial antiport uncoupler FCCP, in association with SS, only then was CHOP expression enhanced. Under these conditions, caspase-3 cleavage/activation was increased two-fold compared with SS alone. Also, cells exposed to CELE had greater caspase-3 activation than cells exposed to SS and undergoing ERSR. These results suggest that CHOP expression and its proapoptotic effect are recruited only under conditions of mitochondrial stress accompanying ERSR. Recruitment of CHOP accompanied augmentation of caspase-3 cleavage, possibly because both ER-associated caspase-4 and mitochondria-driven apoptosis converge on and activate caspase-3, ultimately targeting the cells to apoptosis. FCCP alone

did not increase expression of CHOP or result in caspase-3 cleavage/activation, indicating that some elements of the ERSR cascade are required to induce CHOP expression even in the presence of distressed mitochondria. Although CELE induces ERSR in gastric mucosal cells and in MG cells (Tsutsumi et al., 2004; Pyrko et al., 2007), SS activation of ERSR in glioma cells has not been previously reported. The latter finding could have important implications for translational applications of NSAIDs such as SS.

When MG cells were treated with CELE, upregulation of CHOP, caspase-4 cleavage, and resultant caspase-3 cleavage/activation were all significantly enhanced. At least two mechanisms have been implicated in ERSR-activated cell death: CHOP-directed activation of mitochondrial apoptosis by downregulation of antiapoptotic genes such as *bcl-2* (for review see Oyadomari and Mori, 2004) and GRP78 release, $Ca^{2+}$-calpain-mediated and mitochondria-independent activation of ER-associated caspase-4/12, respectively, in human and murine species (Jiang et al., 2007). The differences between SS and CELE effects on these ERSR-triggered death pathways allowed us to analyze the contribution of these two branches of ERSR on the death of glioma cells during ERSR. Our findings suggest that, in MG cells, SS activates the ERSR death cascade in the absence of CHOP upregulation through unfolded protein-induced GRP78 release of caspase-4 in the presence of calpain-activating elevated $[Ca^{2+}]_i$. Conversely, CELE activates both pathways, causing caspase-4 activation similarly to SS and upregulation of CHOP and larger caspase-3 activation. By targeting the mitochondria with FCCP, SS could act in a manner similar to CELE. However, the toxicity caused by SS and CELE to glioma cells remains similar. This suggests that activation of ER-associated caspases is enough to cause maximal cell death. The additional reinforcement of caspase-3 activation by mitochondrial involvement, as in the case of CELE and SS + FCCP, does not result in additional cell death. The latter finding of ERSR induced death caused by SS in the absence of CHOP induction seems to be a unique feature of MG cells. In fact, in other cell types, such a dependence between mitochondrial damage and CHOP expression induction during ERSR as we observed in MG cells has not been previously described (Oyadomari and Mori, 2004).

Glioma cells exist in a state of chronic ERSR. It has been hypothesized that activation of ERSR allows the cells to survive the harsh environment deriving from cancer overgrowth and be responsible for the fast appearance of resistance to radiotherapy and chemotherapy (Luo et al., 2009; Johnson et al., 2011). We hypothesize that this also curtails the ability of these cells to respond to protein unfolding and may possibly make MG cells susceptible to death induced by additional ERSR induction.

Athough the concentrations of SS and CELE investigated in our study are higher than those typically used to achieve anti-inflammatory, fever-reducing, and antipain effects, they are in agreement with the concentrations reported to be necessary to achieve cancer-preventive or antitumor effects. Because the typical mechanism of action of NSAIDs clearly does not apply to the antiproliferative and antineoplastic effect, it is clear that we are searching for an off-target action of these drugs. Discovery and analysis of these additional effects of NSAIDs, even if they are achieved at high concentrations, may help to identify the mechanism responsible for the antitumor effects. Identification of such a mechanism could lead to the development of programs to optimize the molecules for these specific actions and hence result in a significant reduction of the concentration necessary to elicit the wanted target activation or inhibition.

In conclusion, the present study provides insights regarding the effects of SS and CELE on MG cells. We have shown that SS is a reversible SERCA inhibitor and that CELE, in addition to inhibiting SERCA, causes mitochondrial dysfunction and subsequent $Ca^{2+}$ release from this organelle. Therefore, we propose that, although SS and CELE both are

inducers of ERSR and cytotoxic agents in MG cells, SS selectively induces ERSR and is a more appropriate pharmacophore to target ERSR. The limited inhibition of COX-2 by SS, compared with CELE, could be important when considering adverse and life-threatening side effects. SS also has good bioavailability and crosses the blood–brain barrier. These features make SS a more desirable candidate to explore as a prototype gliotoxic molecule.

## Acknowledgments

GGJ was supported by NIH-NIDA grant # 1R03DA031669 to MG; MCW was supported by grants NIH-NIA # 1R21AG038782 to MG and 1R03DA031669 to MG; MG was partially supported by NIH-NIA # 1R21AG038782 and NIH-NIDA 1R03DA031669 to MG.

## References

Baron JA. Epidemiology of non-steroidal anti-inflammatory drugs and cancer. Prog Exp Tumor Res. 2003; 37:1–24. [PubMed: 12795046]

Bilmen JG, Wootton LL, Godfrey RE, Smart OS, Michelangeli F. Inhibition of SERCA $Ca^{2+}$ pumps by 2-aminoethoxydiphenyl borate (2-APB). 2-APB reduces both $Ca^{2+}$ binding and phosphoryl transfer from ATP, by interfering with the pathway leading to the $Ca^{2+}$-binding sites. Eur J Biochem. 2002; 269:3678–3687. [PubMed: 12153564]

Bootman MD, Collins TJ, Mackenzie L, Roderick HL, Berridge MJ, Peppiatt CM. 2-Aminoethoxydiphenyl borate (2-APB) is a reliable blocker of store-operated $Ca^{2+}$ entry but an inconsistent inhibitor of $InsP_3$-induced $Ca^{2+}$ release. FASEB J. 2002; 16:1145–1150. [PubMed: 12153982]

Cerchietti LC, Bonomi MR, Navigante AH, Castro MA, Cabalar ME, Roth BM. Phase I/II study of selective cyclooxygenase-2 inhibitor celecoxib as a radiation sensitizer in patients with unresectable brain metastases. J Neurooncol. 2005; 71:73–81. [PubMed: 15719279]

Chen ST, Thomas S, Gaffney KJ, Louie SG, Petasis NA, Schonthal AH. Cytotoxic effects of celecoxib on Raji lymphoma cells correlate with aggravated endoplasmic reticulum stress but not with inhibition of cyclooxygenase-2. Leuk Res. 2009; 34:250–253. [PubMed: 19833390]

Chuang HC, Kardosh A, Gaffney KJ, Petasis NA, Schonthal AH. COX-2 inhibition is neither necessary nor sufficient for celecoxib to suppress tumor cell proliferation and focus formation in vitro. Mol Cancer. 2008; 7:38. [PubMed: 18485224]

Cuzick J, Otto F, Baron JA, Brown PH, Burn J, Greenwald P, Jankowski J, La Vecchia C, Meyskens F, Senn HJ, Thun M. Aspirin and non-steroidal anti-inflammatory drugs for cancer prevention: an international consensus statement. Lancet Oncol. 2009; 10:501–507. [PubMed: 19410194]

Egger L, Madden DT, Rheme C, Rao RV, Bredesen DE. Endoplasmic reticulum stress-induced cell death mediated by the proteasome. Cell Death Differ. 2007; 14:1172–1180. [PubMed: 17396132]

Ghosh N, Chaki R, Mandal V, Mandal SC. COX-2 as a target for cancer chemotherapy. Pharmacol Rep. 2010; 62:233–244. [PubMed: 20508278]

Grimaldi M. Astrocytes refill intracellular $Ca^{2+}$ stores in the absence of cytoplasmic [$Ca^{2+}$] elevation: a functional rather than a structural ability. J Neurosci Res. 2006; 84:1738–1749. [PubMed: 17016852]

Grimaldi M, Favit A, Alkon DL. cAMP-induced cytoskeleton rearrangement increases calcium transients through the enhancement of capacitative calcium entry. J Biol Chem. 1999; 274:33557–33564. [PubMed: 10559242]

Grimaldi M, Maratos M, Verma A. Transient receptor potential channel activation causes a novel form of $[Ca^{2+}]_i$ oscillations and is not involved in capacitative $Ca^{2+}$ entry in glial cells. J Neurosci. 2003; 23:4737–4745. [PubMed: 12805313]

Grossman SA, Olson J, Batchelor T, Peereboom D, Lesser G, Desideri S, Ye X, Hammour T, Supko JG. Effect of phenytoin on celecoxib pharmacokinetics in patients with glioblastoma. Neuro Oncol. 2008; 10:190–198. [PubMed: 18287342]

Haak LL, Grimaldi M, Smaili SS, Russell JT. Mitochondria regulate $Ca^{2+}$ wave initiation and inositol trisphosphate signal transduction in oligodendrocyte progenitors. J Neurochem. 2002; 80:405–415. [PubMed: 11905989]

Heytler PG. Uncouplers of oxidative phosphorylation. Methods Enzymol. 1979; 55:462–442. [PubMed: 156853]

Hussain SG, Ramaiah KV. Reduced eIF2alpha phosphorylation and increased proapoptotic proteins in aging. Biochem Biophys Res Commun. 2007; 355:365–370. [PubMed: 17300747]

Jaffe BM. Prostaglandins and cancer: an update. Prostaglandins. 1974; 6:453–461. [PubMed: 4366016]

Jendrossek V, Handrick R, Belka C. Celecoxib activates a novel mitochondrial apoptosis signaling pathway. FASEB J. 2003; 17:1547–1549. [PubMed: 12824303]

Jiang CC, Chen LH, Gillespie S, Wang YF, Kiejda KA, Zhang XD, Hersey P. Inhibition of MEK sensitizes human melanoma cells to endoplasmic reticulum stress-induced apoptosis. Cancer Res. 2007; 67:9750–9761. [PubMed: 17942905]

Johnson AJ, Hsu AL, Lin HP, Song X, Chen CS. The cyclo-oxygenase-2 inhibitor celecoxib perturbs intracellular calcium by inhibiting endoplasmic reticulum $Ca^{2+}$-ATPases: a plausible link with its antitumour effect and cardiovascular risks. Biochem J. 2002; 366:831–837. [PubMed: 12076251]

Johnson GG, White MC, Grimaldi M. Stressed to death: targeting endoplasmic reticulum stress response induced apoptosis in gliomas. Curr Pharm Des. 2011; 17:284–292. [PubMed: 21348829]

Kang YJ, Kim IY, Kim EH, Yoon MJ, Kim SU, Kwon TK, Choi KS. Paxilline enhances TRAIL-mediated apoptosis of glioma cells via modulation of c-FLIP, survivin and DR5. Exp Mol Med. 2011; 43:24–34. [PubMed: 21150246]

Kardosh A, Blumenthal M, Wang WJ, Chen TC, Schonthal AH. Differential effects of selective COX-2 inhibitors on cell cycle regulation and proliferation of glioblastoma cell lines. Cancer Biol Ther. 2004; 3:55–62. [PubMed: 14726653]

Kardosh A, Wang W, Uddin J, Petasis NA, Hofman FM, Chen TC, Schonthal AH. Dimethyl-celecoxib (DMC), a derivative of celecoxib that lacks cyclooxygenase-2-inhibitory function, potently mimics the anti-tumor effects of celecoxib on Burkitt's lymphoma in vitro and in vivo. Cancer Biol Ther. 2005; 4:571–582. [PubMed: 15846081]

Kardosh A, Golden EB, Pyrko P, Uddin J, Hofman FM, Chen TC, Louie SG, Petasis NA, Schonthal AH. Aggravated endoplasmic reticulum stress as a basis for enhanced glioblastoma cell killing by bortezomib in combination with celecoxib or its non-coxib analogue, 2,5-dimethyl-celecoxib. Cancer Res. 2008; 68:843–851. [PubMed: 18245486]

Kesari S, Schiff D, Henson JW, Muzikansky A, Gigas DC, Doherty L, Batchelor TT, Longtine JA, Ligon KL, Weaver S, Laforme A, Ramakrishna N, Black PM, Drappatz J, Ciampa A, Folkman J, Kieran M, Wen PY. Phase II study of temozolomide, thalidomide, and celecoxib for newly diagnosed glioblastoma in adults. Neurooncology. 2008; 10:300–308.

Kim I, Xu W, Reed JC. Cell death and endoplasmic reticulum stress: disease relevance and therapeutic opportunities. Nat Rev Drug Discov. 2008; 7:1013–1030. [PubMed: 19043451]

Koch GL. The endoplasmic reticulum and calcium storage. Bioessays. 1990; 12:527–531. [PubMed: 2085319]

Luo J, Solimini NL, Elledge SJ. Principles of cancer therapy: oncogene and non-oncogene addiction. Cell. 2009; 136:823–837. [PubMed: 19269363]

Moller T. Calcium signaling in microglial cells. Glia. 2002; 40:184–194. [PubMed: 12379906]

Ogata M, Hino S, Saito A, Morikawa K, Kondo S, Kanemoto S, Murakami T, Taniguchi M, Tanii I, Yoshinaga K, Shiosaka S, Hammarback JA, Urano F, Imaizumi K. Autophagy is activated for cell survival after endoplasmic reticulum stress. Mol Cell Biol. 2006; 26:9220–9231. [PubMed: 17030611]

Oyadomari S, Mori M. Roles of CHOP/GADD153 in endoplasmic reticulum stress. Cell Death Differ. 2004; 11:381–389. [PubMed: 14685163]

Piazza GA, Rahm AL, Krutzsch M, Sperl G, Paranka NS, Gross PH, Brendel K, Burt RW, Alberts DS, Pamukcu R, et al. Antineoplastic drugs sulindac sulfide and sulfone inhibit cell growth by inducing apoptosis. Cancer Res. 1995; 55:3110–3116. [PubMed: 7606732]

Pyrko P, Soriano N, Kardosh A, Liu YT, Uddin J, Petasis NA, Hofman FM, Chen CS, Chen TC, Schonthal AH. Downregulation of survivin expression and concomitant induction of apoptosis by celecoxib and its non-cyclooxygenase-2-inhibitory analog, dimethyl-celecoxib (DMC), in tumor cells in vitro and in vivo. Mol Cancer. 2006; 5:19. [PubMed: 16707021]

Pyrko P, Kardosh A, Liu YT, Soriano N, Xiong W, Chow RH, Uddin J, Petasis NA, Mircheff AK, Farley RA, Louie SG, Chen TC, Schonthal AH. Calcium-activated endoplasmic reticulum stress as a major component of tumor cell death induced by 2,5-dimethyl-celecoxib, a non-coxib analogue of celecoxib. Mol Cancer Ther. 2007; 6:1262–1275. [PubMed: 17431104]

Rao CV, Reddy BS. NSAIDs and chemoprevention. Curr Cancer Drug Targets. 2004; 4:29–42. [PubMed: 14965265]

Reardon DA, Quinn JA, Vredenburgh J, Rich JN, Gururangan S, Badruddoja M, Herndon JE 2nd, Dowell JM, Friedman AH, Friedman HS. Phase II trial of irinotecan plus celecoxib in adults with recurrent malignant glioma. Cancer. 2005; 103:329–338. [PubMed: 15558802]

Roe MW, Lemasters JJ, Herman B. Assessment of Fura-2 for measurements of cytosolic free calcium. Cell Calcium. 1990; 11:63–73. [PubMed: 2191782]

Sabala P, Amler E, Baranska J. Intracellular $Ca^{2+}$ signals induced by ATP and thapsigargin in glioma C6 cells. Calcium pools sensitive to inositol 1,4,5-trisphosphate and thapsigargin. Neurochem Int. 1997; 31:55–64. [PubMed: 9185165]

Schonthal AH. Antitumor properties of dimethyl-celecoxib, a derivative of celecoxib that does not inhibit cyclooxygenase-2: implications for glioma therapy. Neurosurg Focus. 2006; 20:E21. [PubMed: 16709027]

Shono T, Tofilon PJ, Bruner JM, Owolabi O, Lang FF. Cyclooxygenase-2 expression in human gliomas: prognostic significance and molecular correlations. Cancer Res. 2001; 61:4375–4381. [PubMed: 11389063]

Shrieve DC, Alexander E, Black PM 3rd, Wen PY, Fine HA, Kooy HM, Loeffler JS. Treatment of patients with primary glioblastoma multiforme with standard postoperative radiotherapy and radiosurgical boost: prognostic factors and long-term outcome. J Neurosurg. 1999; 90:72–77. [PubMed: 10413158]

Tabas I, Ron D. Integrating the mechanisms of apoptosis induced by endoplasmic reticulum stress. Nat Cell Biol. 2011; 13:184–190. [PubMed: 21364565]

Tanaka K, Tomisato W, Hoshino T, Ishihara T, Namba T, Aburaya M, Katsu T, Suzuki K, Tsutsumi S, Mizushima T. Involvement of intracellular $Ca^{2+}$ levels in nonsteroidal anti-inflammatory drug-induced apoptosis. J Biol Chem. 2005; 280:31059–31067. [PubMed: 15987693]

Thastrup O, Foder B, Scharff O. The calcium mobilizing tumor promoting agent, thapsigargin elevates the platelet cytoplasmic free calcium concentration to a higher steady state level. A possible mechanism of action for the tumor promotion. Biochem Biophys Res Commun. 1987; 142:654–660. [PubMed: 2950855]

Thastrup O, Cullen PJ, Drobak BK, Hanley MR, Dawson AP. Thapsigargin, a tumor promoter, discharges intracellular $Ca^{2+}$ stores by specific inhibition of the endoplasmic reticulum $Ca^{2+}$-ATPase. Proc Natl Acad Sci U S A. 1990; 87:2466–2470. [PubMed: 2138778]

Tsutsumi S, Gotoh T, Tomisato W, Mima S, Hoshino T, Hwang HJ, Takenaka H, Tsuchiya T, Mori M, Mizushima T. Endoplasmic reticulum stress response is involved in nonsteroidal anti-inflammatory drug-induced apoptosis. Cell Death Differ. 2004; 11:1009–1016. [PubMed: 15131590]

Tuettenberg J, Grobholz R, Korn T, Wenz F, Erber R, Vajkoczy P. Continuous low-dose chemotherapy plus inhibition of cyclooxygenase-2 as an antiangiogenic therapy of glioblastoma multiforme. J Cancer Res Clin Oncol. 2005; 131:31–40. [PubMed: 15565458]

Wagemakers M, van der Wal GE, Cuberes R, Alvarez I, Andres EM, Buxens J, Vela JM, Moorlag H, Mooij JJ, Molema G. COX-2 inhibition combined with radiation reduces orthotopic glioma outgrowth by targeting the tumor vasculature. Transl Oncol. 2009; 2:1–7. [PubMed: 19252746]

Weiss H, Amberger A, Widschwendter M, Margreiter R, Ofner D, Dietl P. Inhibition of store-operated calcium entry contributes to the anti-proliferative effect of non-steroidal anti-inflammatory drugs in human colon cancer cells. Int J Cancer. 2001; 92:877–882. [PubMed: 11351310]

Xu C, Bailly-Maitre B, Reed JC. Endoplasmic reticulum stress: cell life and death decisions. J Clin Invest. 2005; 115:2656–2664. [PubMed: 16200199]

Yang H, Park SH, Choi HJ, Moon Y. The integrated stress response-associated signals modulates intestinal tumor cell growth by NSAID-activated gene 1 (NAG-1/MIC-1/PTGF-beta). Carcinogenesis. 2010; 31:703–711. [PubMed: 20130018]

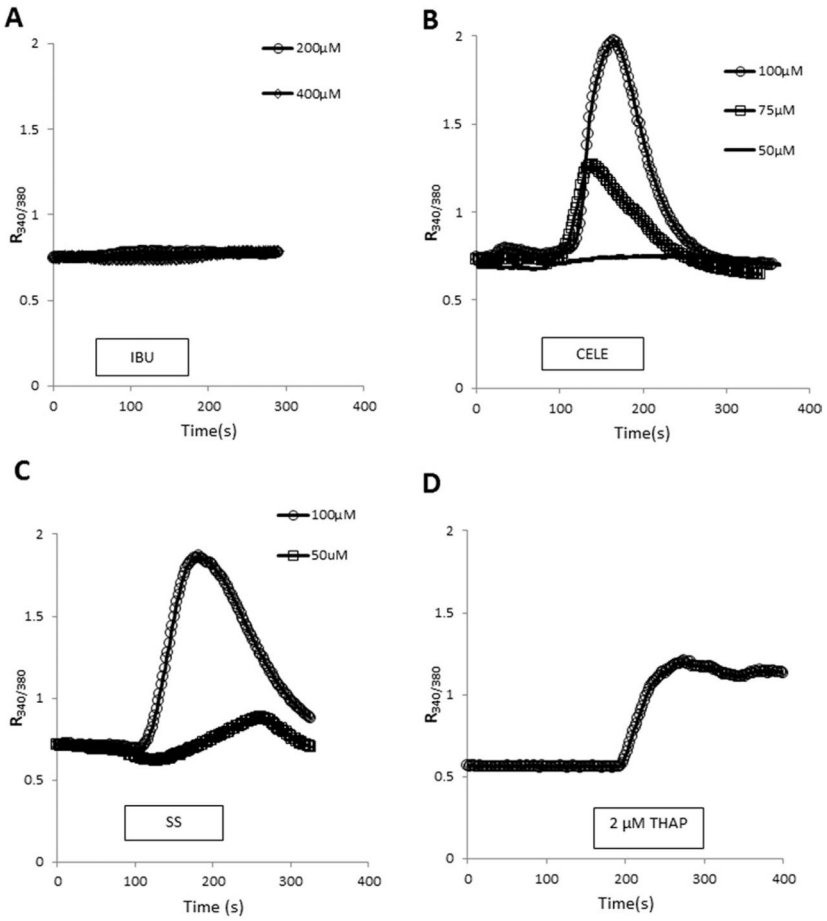


**Fig. 1.**

Effects of NSAIDs on $[Ca^{2+}]_i$. Fura-2-based ratiometric $Ca^{2+}$ imaging experiments were performed on C6 cells. Various test agents were applied, as indicated by the horizontal bars. Line graphs were obtained by averaging data points from all recorded cells in at least three independent preparations obtained from three different cell passages. **A:** IBU, even at high concentrations, had no effect on $[Ca^{2+}]_i$. **B, C:** CELE and SS caused concentration-dependent elevation of $[Ca^{2+}]_i$. The effect of both agents was readily reversible, because the substance-induced $[Ca^{2+}]_i$ elevation subsided upon removing the compounds from the bathing solution. **D:** THAP, 2 μM, shown for comparison, causes the irreversible blockade of SERCA and a $[Ca^{2+}]_i$ elevation. CELE, celecoxib; SS, sulindac sulfide; THAP, thapsigargin; IBU, ibuprofen.

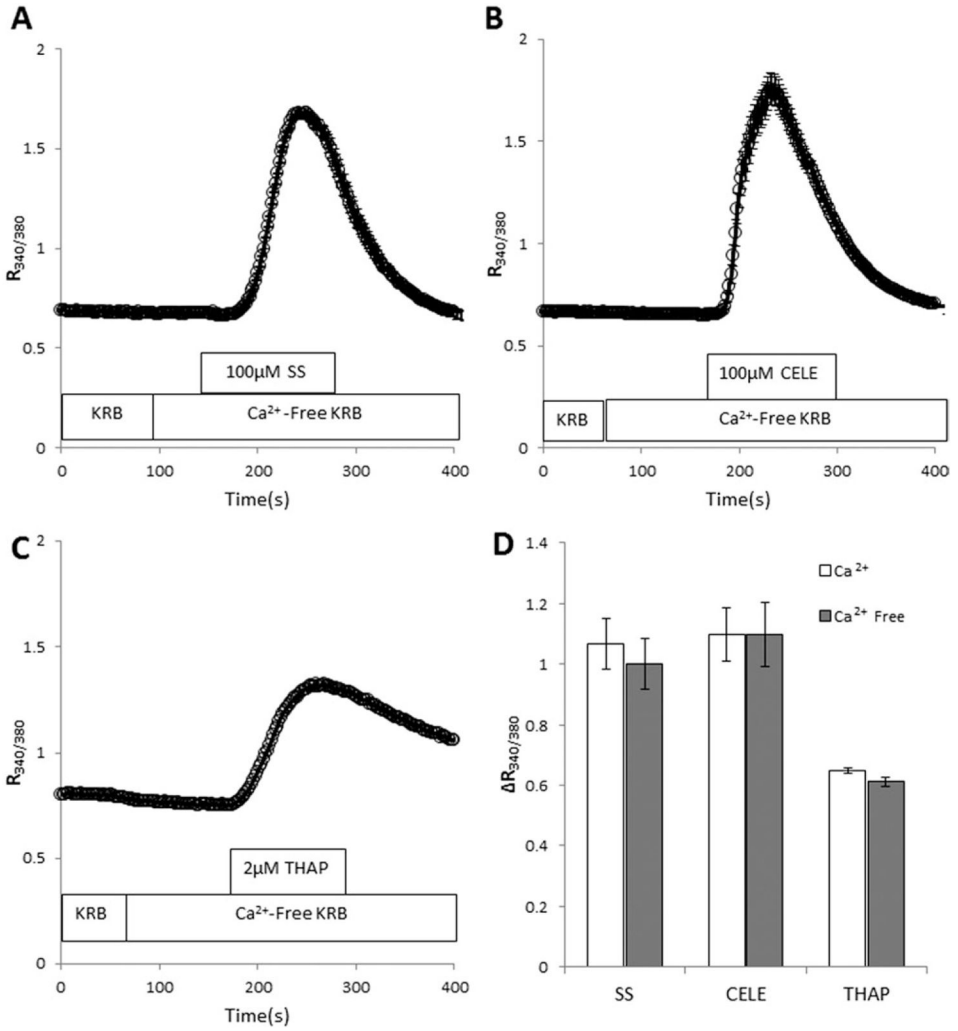


**Fig. 2.**

SS and CELE release $Ca^{2+}$ from intracellular stores without affecting the ion influx from the extracellular environment. SS (**A**) and CELE (**B**), in the absence of extracellular $Ca^{2+}$, increase $[Ca^{2+}]_i$ without any apparent quantitative or qualitative difference compared with their effects in the presence of extracellular $Ca^{2+}$. **C:** The effect of 2 μM THAP is shown for comparison. **D:** The $\Delta Ca^{2+}$ response, expressed as a bar graph, is shown to compare the effect of the agents in the presence and absence of extracellular $Ca^{2+}$. Experiments were performed on three independent cell preparations and passages and included more than 100 cells per treatment. CELE, celecoxib; SS, sulindac sulfide; THAP, thapsigargin.

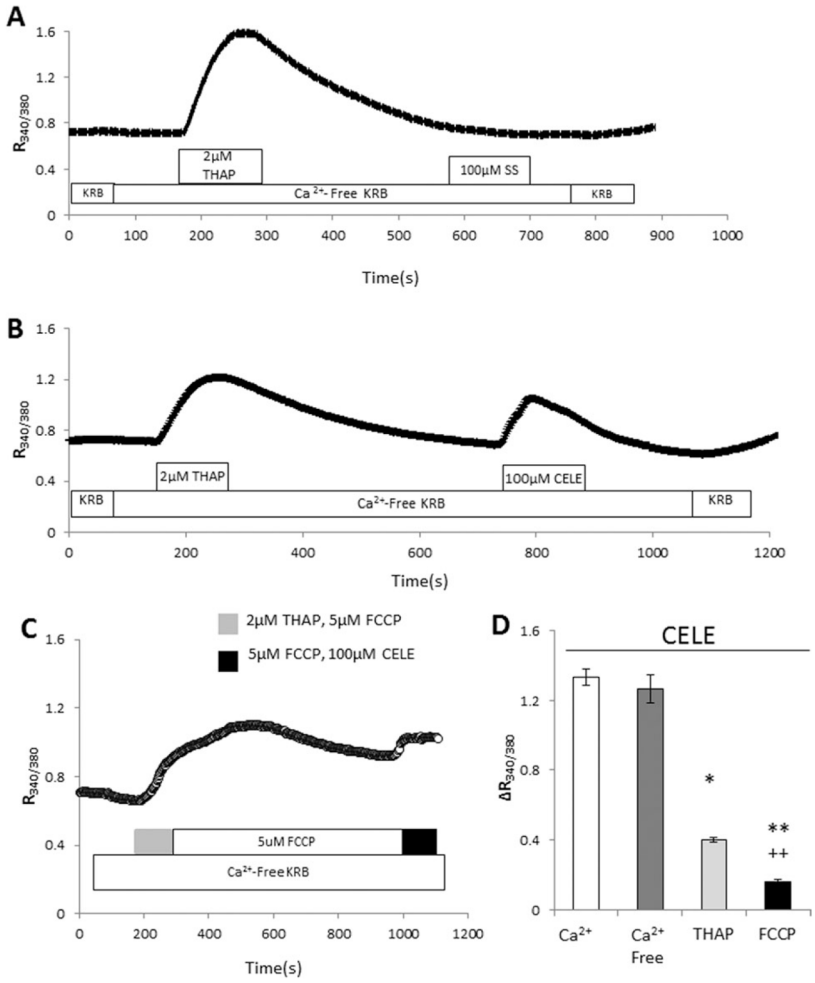


**Fig. 3.**

SS and CELE release $Ca^{2+}$ from a THAP-sensitive store; CELE also releases $Ca^{2+}$ from the mitochondria. **A:** To determine the source of the intracellular $Ca^{2+}$ mobilized by SS and CELE, C6 cells were exposed to the test substances in a $Ca^{2+}$-free solution after THAP exposure to deplete the THAP-sensitive store, namely, the ER. Under these conditions, application of SS did not result in an elevation of $[Ca^{2+}]_i$, indicating that the sole source of $Ca^{2+}$ affected by SS was the THAP-sensitive ER pool. **B:** When similar experiments were performed with CELE, there was a 70% inhibition of the CELE effect, indicating that most of the $Ca^{2+}$ mobilized by CELE was released by a THAP-sensitive pool, namely, the ER. Thus, the residual effect of CELE on $[Ca^{2+}]_i$ must be ascribed to another intracellular $Ca^{2+}$ source. **C:** Mitochondrial poisoning further reduced the effect of CELE. C6 cells were treated in the absence of extracellular $Ca^{2+}$ for 15 min with 2 μM THAP and 5 μM FCCP, to uncouple the proton pump and release $Ca^{2+}$ from the mitochondria. Under these conditions, $Ca^{2+}$ mobilization by CELE was almost completely inhibited, indicating that mitochondria provide the additional source of $Ca^{2+}$ responsible for the CELE effect. **D:** Bar graph reporting the $\Delta Ca^{2+}$ response to CELE in the previous experiments. Imaging experiments were performed on three separate cell preparations and passages and included more than 100 cells per treatment group. $^{*}P \leq 0.05$, $^{**}P \leq 0.01$ vs. $Ca^{2+}$. $^{\dagger\dagger}P \leq 0.01$ vs. THAP. CELE, celecoxib; SS, sulindac sulfide; THAP, thapsigargin; FCCP, carbonyl cyanide 4-(trifluoromethoxy)phenylhydrazone.

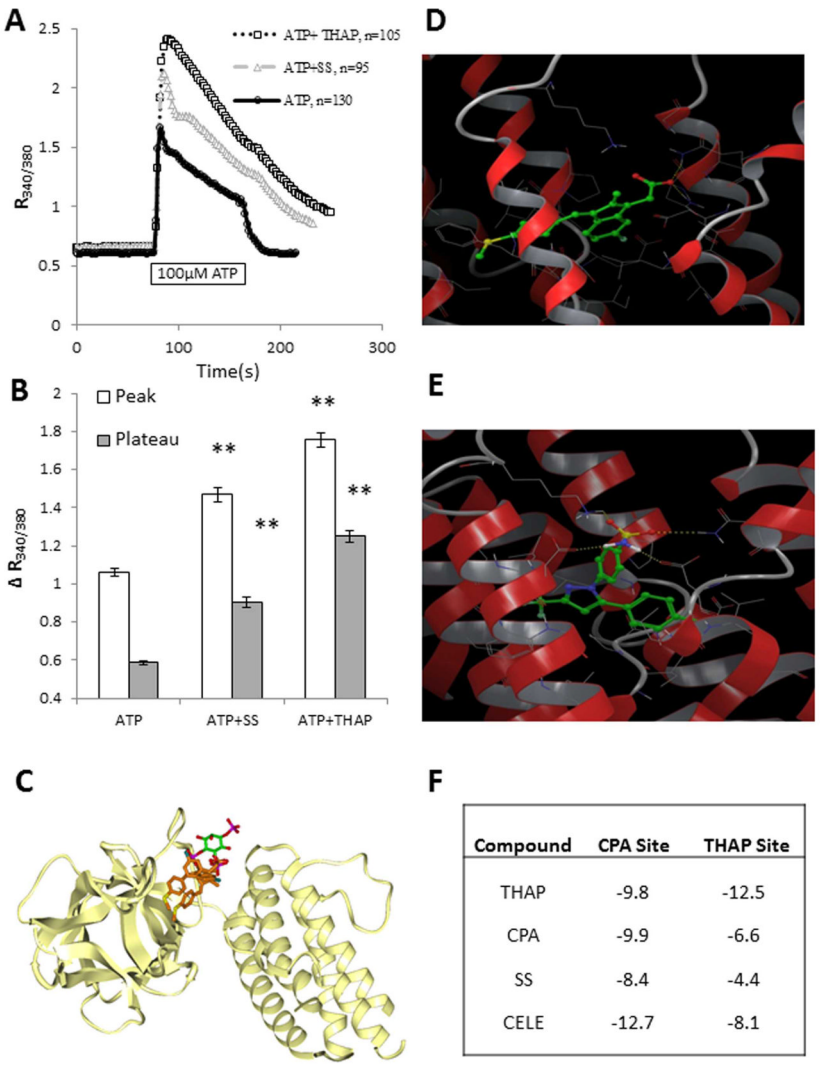


| Compound | CPA Site | THAP Site |
|---|---|---|
| THAP | -9.8 | -12.5 |
| CPA | -9.9 | -6.6 |
| SS | -8.4 | -4.4 |
| CELE | -12.7 | -8.1 |

**Fig. 4.**

SS mobilizes $Ca^{2+}$ from the ER in a THAP-like fashion without affecting the $InsP_3R$. To assess the possible mechanisms of SS-induced $Ca^{2+}$ mobilization from the ER, C6 cells were exposed to the maximal ATP concentration in the presence of SS or THAP. **A:** SS added simultaneously with ATP causes a change in the ATP response profile similar to that of THAP. $Ca^{2+}$ mobilization in response to ATP in the presence of SS shows an increase in the peak response to the already maximal $InsP_3$ effect elicited by ATP. These results indicate that SS affects a target other than the $InsP_3R$. In addition to potentiation of the ATP peak response, there is also an increase in the length and levels of the plateau phase of the response. The latter could be a result of increased $Ca^{2+}$ influx, but most likely is due to the failure of ER uptake mechanisms, because there was no effect on $Ca^{2+}$ influx by SS. These data indicate that SERCA is a potential target of SS. **B:** Differences in the peak and plateau phases are represented in bar graphs following treatment of cells with ATP, ATP + SS, or ATP + THAP. The peak values represent the highest values recorded following ATP exposure (usually reached within 4–6 sec); plateau values represent $Ca^{2+}$ values 40 sec after ATP challenge. ATP + SS and ATP + THAP treatments resulted in higher peak and plateau phases than treatment with ATP alone. Experiments were performed on three or more independent cell preparations and passages, with more than 90 cells analyzed per treatment

group. $^{**}P \leq 0.01$ vs. ATP alone corresponding values. **C:** Two possible fitted structures of SS in the active site of the $InsP_3R$ illustrate that the available site is exposed to the solvent. SS carbon atoms are light brown. The position of the cocrystallized $InsP_3$, with green carbons, is shown for comparison. **D:** The structural details of the docked results for SS are highlighted. **E:** Structural details of the docked results for CELE are shown. In D and E, SERCA is represented as a ribbon with residues close to (<5 Å) docked compounds explicitly shown. SS and CELE are represented as sticks with green carbon atoms. Noncarbon atoms are red (O), blue (N), yellow (S), or white (H). Intermolecular hydrogen bonds are marked with dashed lines. **F:** The calculated binding energies (docking scores) associated with the binding poses are shown in the table. More negative values indicate tighter binding affinities. CELE, celecoxib; SS, sulindac sulfide; THAP, thapsigargin; $InsP_3R$, inositol triphosphate receptors. [Color figure can be viewed in the online issue, which is available at wileyonlinelibrary.com.]

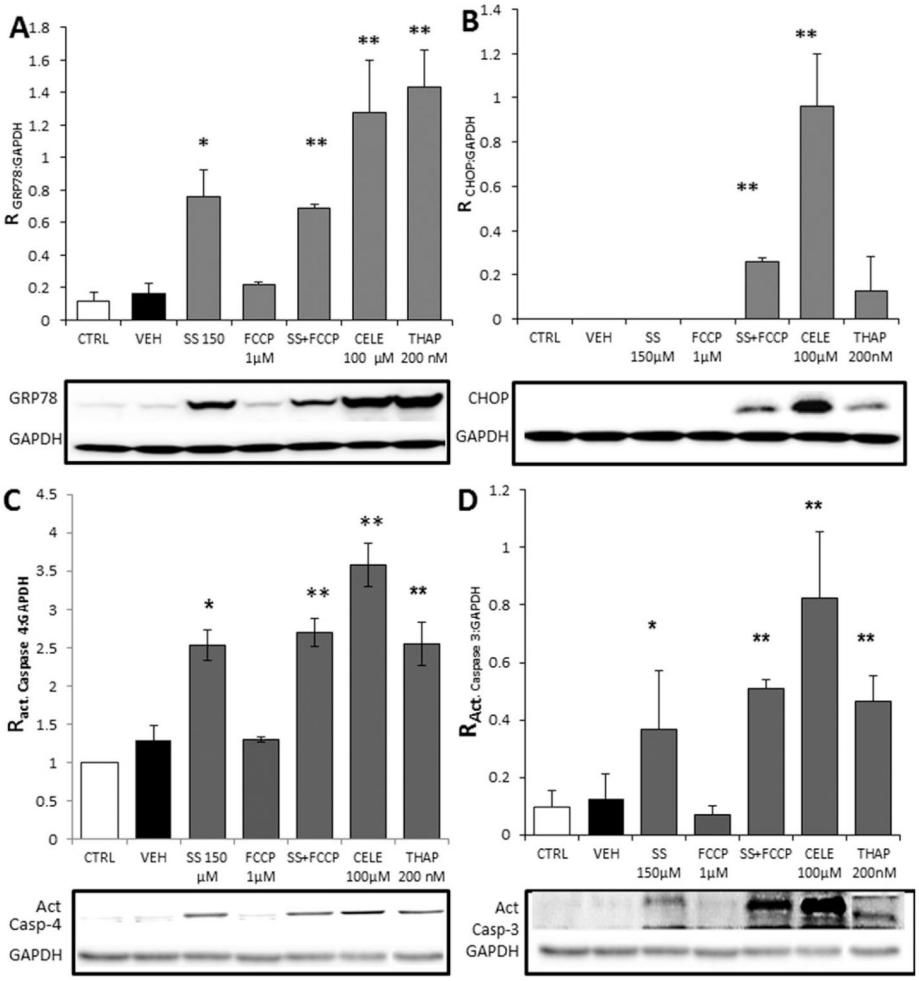


**Fig. 5.**

Exposure to NSAIDs results in different patterns of ERSR activation in human glioma cells. **A:** MG cells were exposed to SS, CELE, THAP, or FCCP for 18 hr, and expression of ERSR-associated proteins was assessed by quantitative Western blots. Analysis of GAPDH-normalized GRP78 expression showed that SS and SS + FCCP caused a similar 4.5-fold induction (FOI) of GRP78 expression, whereas CELE and THAP caused 7.5 and 8 FOI, respectively. **B:** The expression of CHOP in MG cells was increased only by CELE and SS + FCCP, indicating that CHOP upregulation, during ERSR, requires mitochondrial damage. Treatment with 1 μM FCCP failed to increase CHOP expression, showing that mitochondrial poisoning alone does not increase CHOP expression. **C:** A 24-hr treatment with 150 μM SS, 100 μM CELE, 200 nM THAP, or 150 μM SS + 1 μM FCCP increased caspase-4 cleavage/activation in U-87 MG cells by 2.5–3 FOI. Ratio (R) of caspase 4 was calculated by dividing cleaved caspase 4 by GAPDH and compared with control. These findings, combined with the data obtained on CHOP, confirmed that NSAIDs cause activation of ER-associated caspases independently of mitochondrial involvement. **D:** Caspase-3 activation was increased in U-87 MG cells exposed to 150 μM SS, 100 μM CELE, 200 nM THAP, or 150 μM SS + 1 μM FCCP for 24 hr. FCCP alone did not cause caspase-3 activation. In contrast to caspase-4 activation, caspase-3 activation was increased by simultaneous ERSR activation and mitochondrial poisoning. SS alone caused a 4.1 FOI, SS + FCCP a 5.5 FOI, CELE a 9.1 FOI, and THAP 5.1 a FOI of caspase-3 activation. Ratio

(R) of caspase-3 was calculated by dividing cleaved caspase-3 by GAPDH and compared with control. The potentiation of capase-3 activation observed in the cells treated with SS + FCCP and CELE indicates that mitochondrial poisoning and the resulting CHOP upregulation participate in further caspase-3 activation, explaining why the CELE effect on caspase-3 is greater than that of SS alone but similar to that for SS + FCCP. Data points in each panel represent averages from three separate experiments performed on three independent cell preparations and passages. $*P < 0.05$ compared with the values for CTRL and VEH. $**P \leq 0.01$ compared with the values for CTRL and VEH. CELE, celecoxib; SS, sulindac sulfide; THAP, thapsigargin; FCCP, carbonyl cyanide 4-(trifluoromethoxy)phenylhydrazone.

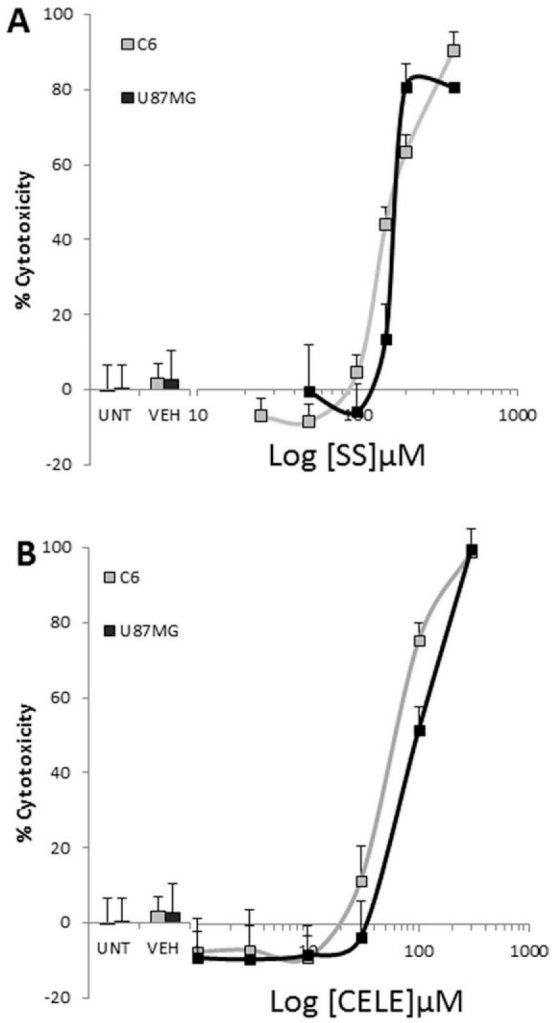


**Fig. 6.**

NSAIDs are toxic to glioma cells. **A:** MG and C6 cells were treated for 48 hr with graded concentrations of SS and assessed for viability with Cell Titer Glo. SS caused a concentration-dependent cytotoxic effect on MG cells. The maximal effect was reached at 200 μM, at which concentration more than 85% of the cells were dead. A similar maximal effect was recorded for C6 cells. Nearly 100% toxicity occurred at the highest SS concentration tested. **B:** CELE toxicity was similar for C6 and MG cells. At 300 μM, CELE reduced viability of both cell lines by >99%. Experiments were performed in quadruplicate on three independent cell preparations and passages. Curves were obtained by pooling the results from all experiments, and results were analyzed via *t*-test. CELE, celecoxib; SS, sulindac sulfide.